

Quantitative multiple-scattering analysis of near-edge x-ray-absorption fine structure: $c(2 \times 2)O$ on $Cu(100)$

D. D. Vvedensky and J. B. Pendry

The Blackett Laboratory, Imperial College, London SW7 2BZ, United Kingdom

U. Döbler* and K. Baberschke

*Institut für Atom- und Festkörperphysik, Freie Universität Berlin,
D-1000 Berlin 33, Federal Republic of Germany*

(Received 2 March 1987)

The structure of $c(2 \times 2)O$ on $Cu(100)$ is investigated with a full multiple-scattering analysis of the near-edge x-ray-absorption fine structure (NEXAFS). Various adsorption sites and bond lengths are tested, with the oxygen overlayer found to occupy fourfold hollow sites 0.7 ± 0.1 Å above the Cu surface plane, in agreement with recent surface extended x-ray-absorption fine-structure (SEXAFS) work on the same sample. Our study provides the first demonstration that a quantitatively accurate NEXAFS analysis is attainable with low-noise high-resolution data, and opens up new possibilities for surface analysis for those cases where SEXAFS is not applicable.

Surface x-ray-absorption spectroscopy has emerged as a powerful technique for determining the local geometry of atomic and molecular adsorbates. At high energies, surface extended x-ray-absorption fine structure (SEXAFS) yields bond lengths directly from standard Fourier-transform methods, while atomic adsorption sites may frequently be inferred from the polarization dependence of SEXAFS amplitude ratios. However SEXAFS has some severe limitations: (i) the technique is difficult to apply to systems with many edges within the first 300 eV of the SEXAFS range (e.g., N and C *K*-edge SEXAFS for NO and CO, or O *K*-edge SEXAFS on Ag because of the substrate *M* edges), and (ii) for submonolayer coverages, SEXAFS may have sensitivity problems. Nearer to threshold, the longer mean free path and consequent multiple scattering (MS) of the photoelectron enhance the sensitivity of the x-ray-absorption near-edge structure (XANES, or NEXAFS) to the local environment of the excited atom, and produce large modulations of the absorption cross section as a function of photon energy. Moreover, both of the aforementioned difficulties with SEXAFS may be overcome with a MS analysis of NEXAFS because (i) a range of photon energies extending only to 50 eV above the edge is required, and (ii) the larger amplitudes mean greater signal-to-noise ratios for NEXAFS as compared with SEXAFS.

Nevertheless, relatively little effort has been put into extracting structural information for atomic adsorbates from NEXAFS, a notable exception being the pioneering work of Norman *et al.*¹ In this Rapid Communication we show that an MS analysis of the low-noise high-resolution NEXAFS now obtainable can yield not only the adsorption site as in Ref. 1, but also the adsorbate-substrate interlayer spacing to an accuracy of ± 0.1 Å. We consider the $c(2 \times 2)$ phase of O on $Cu(100)$ as an example.

The chemisorption system O on $Cu(100)$ is intriguing because despite an apparent simplicity and tantalizing

similarity to O/Ni(100), numerous experimental studies (see Refs. 2 and 3, and references therein) have yielded conflicting geometries for the $c(2 \times 2)$ superstructure. Indeed, the recent low-energy electron diffraction LEED work of Mayer, Zhang, and Lynn² has questioned even the existence of the $c(2 \times 2)$ phase and favors instead the formation only of the $(\sqrt{2} \times \sqrt{2})R45^\circ$ superstructure. We will analyze the O *K*-edge NEXAFS for the $(\sqrt{2} \times \sqrt{2})R45^\circ$ superstructure in a later publication.

In a recent SEXAFS study of $c(2 \times 2)O$ on $Cu(100)$, Döbler, Baberschke, Stöhr, and Outka³ found a fourfold hollow adsorption site with a nearest-neighbor bond length of 1.94(4) Å, which corresponds closely to the $c(2 \times 2)O/Ni(100)$ structure.⁴ We present below an MS analysis of the corresponding NEXAFS measurements to test the structure deduced from SEXAFS. We calculate absorption spectra for the $c(2 \times 2)$ phase with fourfold hollow, bridge, and atop oxygen adsorption sites with the SEXAFS bond length, and then calculate the effects of bond-length variations for the fourfold hollow site. The low noise and high resolution of the measured data facilitate for the first time a *quantitative* MS NEXAFS analysis. We find that oxygen in the $c(2 \times 2)$ overlayer occupies fourfold hollow sites, with an O-Cu interlayer spacing of 0.7 ± 0.1 Å, corresponding to an O—Cu bond length of ≈ 1.9 Å, in remarkable agreement with the SEXAFS study.³

The experiments were performed at the Berliner Elektronenspeicherring-Gesellschaft für Synchrotronstrahlung (BESSY) using the SX-700 monochromator. Spectra were recorded for polar angles of $\theta=20^\circ$ and $\theta=90^\circ$, where θ is the angle between the electric field vector **E** and the surface normal, under partial-electron-yield conditions. The spectra of the covered sample were divided by those of the clean sample, with the first point of the data set to unity. During the SEXAFS experiments special scans with a step width of approximately 0.5 eV were made for the near-edge structure under the same condi-

tions as in Ref. 3. Substrate preparation, exposure to O₂, and subsequent superstructure formation are also described in Ref. 3.

The calculations were carried out with the program ICXANES⁵ with all calculations having been checked for convergence in angular momentum and cluster size. For an energy-independent 1-eV imaginary part of the constant potential, convergence for all geometries was achieved by including atoms up to a radial distance of 5.5–6.0 Å from the excited atom, i.e., 8 oxygen atoms, and 54, 34, and 46 copper atoms for the hollow, bridge, and atop sites, respectively. The potential was constructed by superposing neutral O and Cu charge densities⁶ in the crystalline Cu₂O structure (the SEXAFS standard). Complex O and Cu phase shifts were then generated by integrating the Schrödinger equation along a contour whose imaginary part is the absorptive part of the constant potential (1 eV). The resulting Cu phase shifts produced an excellent fit to the crystalline Cu *K*-edge NEXAFS. Several other potentials were constructed, e.g., from the CuO crystal structure, with all prescriptions leading to substantially similar spectra to those presented here.

In Fig. 1 we compare the experimental O *K*-edge NEXAFS for *c*(2×2)O on Cu(100) with full MS calculations for the fourfold hollow, bridge, and atop adsorption sites. The structural parameters include the SEXAFS value for the O—Cu bond length³ and the truncated crystal structure for the substrate (*a* = 3.615 Å). All calculated spectra have been folded with a room-temperature Fermi function and the calculated and measured NEXAFS have

been aligned to highlight the accuracy of the calculations in accounting for relative peak positions for the determined geometry.

We see that the calculations only for the fourfold hollow site are compatible with the measured spectra. The relative intensities are in generally good agreement with the experimental profiles for both polarizations and for $\theta=90^\circ$ polarization, the relative peak positions are reproduced to within 0.5 eV. On the other hand, the comparison of peak positions for $\theta=20^\circ$ is not as striking, which is due in part to the absence of a surface barrier in our calculations and the resulting loss of photoelectron current into the vacuum for energies below the work function.

To assess the importance of MS, we have also compared in Fig. 1 the full MS calculations for each adsorption site with the corresponding curved-wave single-scattering (SS) calculation. The dominant features and overall profile in the MS spectra for $\theta=20^\circ$ are well reproduced beyond 10 eV past threshold, though the resolution of structure nearer the edge is lost. In contrast, for $\theta=90^\circ$ there are measurable discrepancies between the two calculations even 30 eV above the edge. Nevertheless, the general profile of the SS calculation is in qualitative agreement with the MS spectrum.

In Fig. 2 we compare the measured NEXAFS for $\theta=20^\circ$ polarization with full MS calculations for the fourfold hollow site at five perpendicular O—Cu interlayer spacings: $d_\perp = 0.5, 0.6, 0.7, 0.8,$ and 0.9 Å. As expected, the calculated spectra for $\theta=90^\circ$ are relatively insensitive to d_\perp for this range of values, and so will not be considered further. The *multiple scattering* peak at 3 eV from

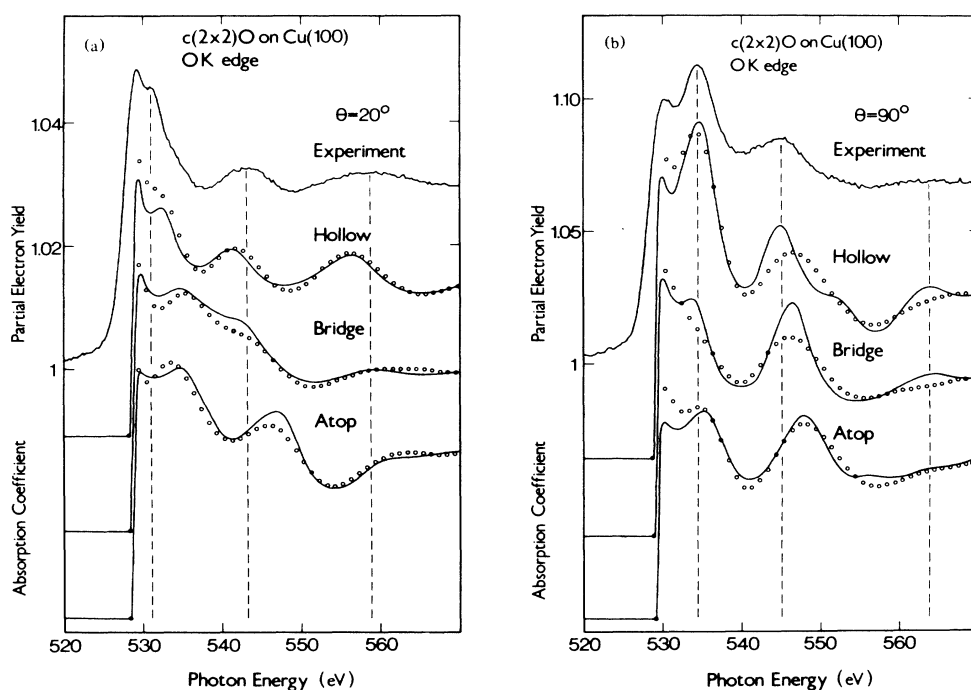


FIG. 1. Comparison of measured O *K*-edge NEXAFS of *c*(2×2)O on Cu(100) for $\theta=20^\circ$ and $\theta=90^\circ$ with full MS (solid lines) and SS (open circles) calculations for the fourfold hollow, bridge, and atop adsorption sites. The reduced edge jump for the $\theta=20^\circ$ NEXAFS is due to the larger background in the pre-edge regime.

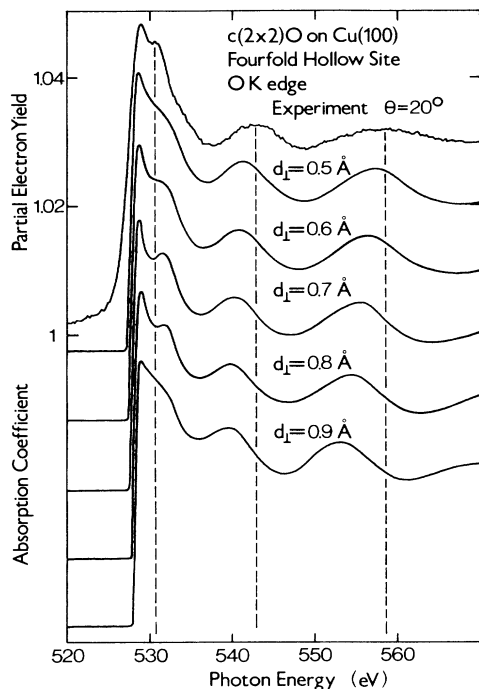


FIG. 2. Comparison of measured O *K*-edge NEXAFS of $c(2\times 2)$ O on Cu(100) for $\theta=20^\circ$ with full MS calculations for the indicated O-Cu interlayer spacings.

$d_\perp=0.7$ Å evolves into a shoulder for $d_\perp=0.6$ Å and becomes less pronounced for $d_\perp=0.8$ Å, before disappearing for $d_\perp\geq 0.9$ Å and $d_\perp\leq 0.5$ Å. The calculations with $d_\perp=0.6, 0.7,$ and 0.8 Å thus offer the best overall agreement with the measured NEXAFS. Our results are consistent with normal photoelectron diffraction studies,⁷ which found the fourfold hollow adsorption site with $d_\perp=0.8$ Å. Other determinations of adsorption geometry and d_\perp are clearly incompatible with Figs. 1 and 2.

To show that changes in isolated features of calculated NEXAFS can have structural significance in wider contexts, we compare in Fig. 3 the measured O *K*-edge NEXAFS for (2×1) O on Ni(110) with MS and SS calculations for an unreconstructed substrate and for several models of adsorbate-induced reconstruction. Note that the SS calculations are again largely insensitive to the structural modifications considered. Although the model with an unreconstructed substrate may be eliminated immediately, the only distinguishing feature of the calculated NEXAFS for the models with reconstructed substrates is the amplitude of the peak at 539 eV, which is virtually absent in the measured NEXAFS. The structural significance of this feature derives from identifying the pertinent MS paths for each structure,^{8,9} which are shown in the inset. The successively diminished prominence of the associated peak in passing from the missing row to the sawtooth model, and then allowing a 20° tilt of oxygen toward the (100) facets is associated in the first instance with a reduction in the number of the identified paths and second with a decrease in the amplitude resulting from shadowing by intervening substrate atoms. Thus, of the

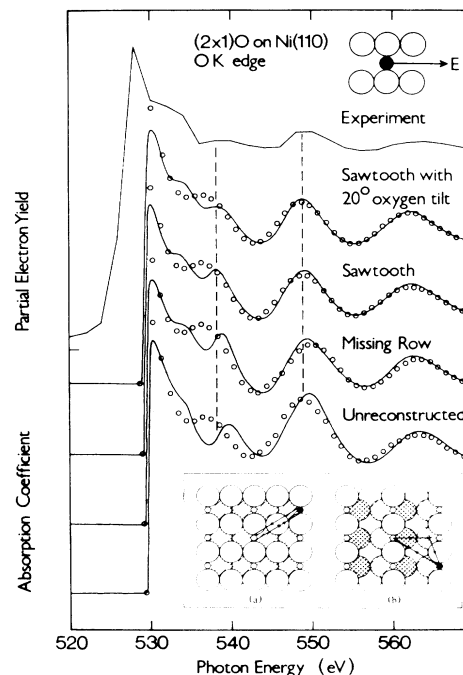


FIG. 3. Comparison of measured O *K*-edge NEXAFS of (2×1) O on Ni(110) for the indicated polarization in the substrate plane with full MS (solid lines) and SS (open circles) calculations for an unreconstructed substrate and for several models of reconstruction. Inset: the important MS paths for (a) the unreconstructed substrate and (b) reconstructed substrates. Large and small open circles represent Ni and O atoms, respectively; hatched circles represent second-layer Ni atoms, with those absent in the sawtooth model indicated by double hatching. For each MS path, the backscattering O atom has been darkened, and the intermediate Ni scattering center indicated by a cross.

three likely models of oxygen-induced reconstruction (see Ref. 10, and references therein), the comparisons in Fig. 3 support the sawtooth model with an appreciable oxygen tilt, again in agreement with SEXAFS.¹⁰

To summarize, the most important aspect of this work is the demonstration that certain detailed structural features of local adsorbate environment are accessible from NEXAFS *provided* the pertinent MS paths have been identified. We are thereby able to demonstrate explicitly for simple systems the quantitative complementarity between SEXAFS and NEXAFS. In more complex cases NEXAFS may be used to probe several candidate structural models revealed by SEXAFS at a much greater level of detail than would be possible from a less discriminating MS analysis.

Although the NEXAFS analysis for $c(2\times 2)$ O on Cu(100) was carried out with prior knowledge of the SEXAFS results, the procedure for an unknown system would be the same. (1) SS analysis to determine site geometry, followed by (2) MS analysis of grazing-incidence data to determine d_\perp , and (3) self-consistent MS check with normal-incidence data. Comparisons between theory and experiment similar to those reported

here have been carried out for $(2 \times 1)O$ on Cu(110) (Ref. 9) and near-edge structure analyses of more complex systems, i.e., hydrocarbons on copper surfaces are under current investigation.

The support of the Bundesminister für Forschung und Technologie under Grant No. 050233 BB is gratefully acknowledged.

*Present address: Siemens, Systemtechnik, Nonnendamm 101, D-1000 Berlin 13, Federal Republic of Germany.

¹D. Norman, J. Stöhr, R. Jaeger, P. J. Durham, and J. B. Pendry, *Phys. Rev. Lett.* **51**, 2052 (1983).

²R. Mayer, C.-S. Zhang, and K. G. Lynn, *Phys. Rev. B* **33**, 8899 (1986).

³U. Döbler, K. Baberschke, J. Stöhr, and D. A. Outka, *Phys. Rev. B* **31**, 2532 (1985).

⁴J. Stöhr, R. Jaeger, and T. Kendelewicz, *Phys. Rev. Lett.* **49**, 142 (1982).

⁵D. D. Vvedensky, D. K. Saldin, and J. B. Pendry, *Comput. Phys. Commun.* **40**, 421 (1986).

⁶E. Clementi and C. Roetti, *At. Data Nucl. Data Tables* **14**, 177 (1974).

⁷J. G. Tobin, L. E. Klebanoff, D. H. Rosenblatt, R. F. Davis, E. Umbach, A. G. Baca, D. A. Shirley, Y. Haung, W. M. Kang, and S. Y. Tong, *Phys. Rev. B* **26**, 7076 (1982).

⁸D. D. Vvedensky and J. B. Pendry, *Phys. Rev. Lett.* **54**, 2725 (1985); D. D. Vvedensky and J. B. Pendry, *Surf. Sci.* **162**, 903 (1985).

⁹U. Döbler, K. Baberschke, D. D. Vvedensky, and J. B. Pendry, *Surf. Sci.* **178**, 679 (1986).

¹⁰K. Baberschke, U. Döbler, L. Wenzel, D. Arvanitis, A. Barattoff, and K. H. Rieder, *Phys. Rev. B* **33**, 5910 (1986).